REVISTA MATÉRIA V.24 N.04
ISSN 1517-7076 articles e-12489, 2019

Influence of doping with Sm3+ on photocatalytic reuse of ZnO thin films obtained by spin coating

Nivaldo Freire de Andrade Neto[1], Raquel Guilherme de Carvalho[1], Laurênia Martins Pereira Garcia[1], Rubens Maribondo Nascimento[1], Carlos Alberto Paskocimas[1], Elson Longo[2], Maurício Roberto Bomio Delmonte[1], Fabiana Villela da Motta[1].

[1] LSQM, DEMAT, UFRN, Av. Sen. Salgado Filho, 3000, Natal, RN, Brasil.
[2] LIEC, DQ, UFSCar, Via Washington Luiz, km 235, CEP 13565-905, São Carlos, SP, Brazil.
e-mail: nfandraden@gmail.com

ABSTRACT

The difficulty in the powder reuse favors the study of materials in the form of thin films. ZnO based films have high photocatalytic potential. In this work, ZnO:xSm3+ (x = 0, 1, 2 and 4 %mol) thin films were prepared by spin coating method. The resins obtained to manufacture the thin films were prepared by complex polymerization method. The samples were characterized by X-ray diffraction (XRD), atomic force microscopy (AFM), field emission scanning electron microscopy (FE-SEM) and spectroscopy UV-Vis. XRD patterns indicate that doping with 4%Sm forms Sm2O3 as the secondary phase. FE-SEM images of the cross section of thin films indicated a uniform thickness ranging from 354 to 367 nm between samples. The incorporation of Sm3+ ions in the ZnO lattice increases the Egap of the films. The photocatalytic performance of the films was tested with the photodegradation of methylene blue dye. Pure ZnO and ZnO:1%Sm3+ exhibited the best activity in the photodegradation. Thin films of pure ZnO exhibit the best photocatalytic results for the first cycle, but considerably reduce their efficiency with reuse. Sm3+ incorporation, without secondary phase formation, was efficient for the maintenance of the photocatalytic property after 3 cycles.

Keywords: Samarium doped zinc oxide; spin coating; thin films; photocatalytic reuse.

1.INTRODUCTION

In recent years, semiconducting oxide photocatalysts, such as zinc oxide (ZnO), have increasingly received high attentions as the materials offer great potentials in the degradation of various environmental pollutants [1, 2], such as pesticides, heavy metals and dyes [3, 4]. In addition, the ZnO is known as one of the most important active photocatalysts due to its advantages, including high initial activity rates, many active sites with high surface reactivity, low price and environmental safety [5]. However, the photocatalytic activity of ZnO is limited to the ultraviolet region and the rapid recombination of photocatalytic loads (h+/e-) decreases the efficiency of the process, making it unfavorable to use as commercial ZnO photocatalyst [6]. Recently, it has been reported that doping of rare earth ions on ZnO improves photocatalytic performance [5]. Some studies have reported that rare earth ions are useful, since rare earth ions produce energy levels of impurities in the gap and their response to visible light. In addition, photogenerated charge carriers are produced, thus accelerating the interfacial transfer of the charge and inhibiting the recombination of the electron-hole pairs [7, 8].

The ZnO powder catalysts show tendency to be difficult to recover and recycle. One substitutive form is thin films of ZnO which comprises dispersed immobilized ZnO particles or layers on a surface [2]. The ZnO thin films can be manufactured by various techniques, such as pulsed laser deposition (PLD) [9], molecular beam epitaxy (MBE) [10], chemical vapor deposition [11], sol gel process [12], spray pyrolysis [13] and Pechini [14]. Although physical methods have been widely used in thin film technology, chemical methods such as the Complex Polymerization Method (CPM) produce low-cost, simple and highly controlled films [15].

In this study, the effect of the photocatalytic properties of ZnO:xSm3+ (x = 0, 1, 2 and 4 %mol) thin

Corresponding Nivaldo Freire Andrade Neto Received on: 11/11/2018 Accepted on: 22/04/2019

10.1590/S1517-707620190004.0814

films produced by the resin obtained by CPM was evaluated. The thin films were characterized by X-ray diffraction (XRD), UV-Vis spectroscopy, field emission scanning electron microscopy (FEG-SEM) and atomic force microscopy (AFM). The methylene blue dye was used in the degradation test is a batch of product in the textile industry. Three photocatalytic tests were performed without any treatment on the film.

2.MATERIALS AND METHODS

Polymer resins were prepared using citric acid/metal cations in the ratio of 6:1. Ethylene glycol was added in a ratio of 40/60 (%mass) relative to citric acid, keeping this constant value in all compositions. Firstly, Citric acid (C6H8O7.H2O) and Zn(NO3)2.6H2O were dissolved in 80 mL of water under stirring at 70°C, ethylene glycol was added after 1 hour and the temperature was raised to 90°C to form a homogeneous and transparent resin. The samarium resins were obtained in a similar form, where samarium nitrate was added stoichiometrically in the molar ratios of 1, 2 and 4%.

Before the deposition of the resin, silicon substrates (0.7 cm x 0.7 cm) underwent two-step cleaning, were first washed in ultrasonic bath in isopropyl alcohol and distilled water. The substrates were dried directly in spin coating. The polymeric precursor was then deposited on the substrates by spin coating to 7000 rpm for 30 sec, four layers being deposited. For each deposited layer was annealed at 350°C for 1 hour and 700°C for 2h at a heating rate of 1oC/minute in air.

The thin films were characterized by XRD using a Shimadzu diffractometer (Model XRD-7000, CuK radiation (λ = 1.54 Å), 40 kV and 30 mA and 2θ from 30° to 40°. The morphology was observed by SEM (Carl Zeiss Supra 35 VP-Model, Germany). Surface of the thin films was investigated by atomic force microscope (AFM). The reflectance of the films was obtained by the UV–Vis–NIR spectrophotometer (Shimadzu, UV 2600) over the spectral wavelength ranges from 200 nm to 900 nm. All the measurements were taken at room temperature. The total amount of organic carbon was used for mineralization analysis. For this, the TOC analyzer Shimadzu 500 was used.

Photocatalytic properties of ZnO:xSm3+ thin films (x = 0, 1, 2 and 4 %mol) were evaluated by measuring the photodegradation of MB (methylene blue) dye with a molecular formula C16H18N3SCl (99.5% purity) in an aqueous solution were illuminated by UVC lamps (Philips TUV 15 W, with maximum intensity at 254 nm = 4.9 eV). Samples with dimensions of 0.7 cm2 were placed in a quartz cell under visible light MB containing solution (1x10-5 mol.L-1). These suspensions were 1 hour in contact MB dye before the test is to allow the saturated absorption of MB onto the catalyst. The variations of the maximum absorption band of supernatant solutions were monitored at intervals of 30 minutes by UV-visible absorbance spectra measurements using a Shimadzu (UV-2600 model) spectrophotometer. The absorbance variation was observed for 420 minutes. All measurements were taken at room temperature. The reuse occurred in a similar manner to that described above, where after each cycle the thin films were air dried and the aqueous solution of MB (1x10-5 mol.L-1) was replaced with the aqueous solution of 420 minutes. The photodegradation was calculated by the equation 1 [9], given below:

$$\% \text{ of MB} = (Co-C)/Co \quad (1)$$

Where: C0 is the concentration of MB before irradiation (concentration of MB after 1 hour adsorption in dark) and C is the concentration of MB after the irradiation certain team.

3.RESULTS

Fig. 1 shows the XRD patterns obtained for the thin films of ZnO:xSm^{3+} (x = 1, 2 and 4 %mol). All thin films show the characteristic peaks of ZnO layer type structure with hexagonal Wurtizita (JCPD 36-1431) were three diffraction peaks are related to reflection planes (100), (002) and (101). Thin films of ZnO:xSm with x = 1 and 2% did not present the formation of secondary phases. The presence of Sm_2O_3 phase was observed in ZnO:4%Sm thin film. According to Fig. 1, it is observed that the incorporation of Sm^{3+} in the ZnO lattice provides a shift of the peaks to smaller angles, indicating that the doping occurred successfully. The shift in the peaks occurs due to the difference between the ionic radius of the cations, being 0.096 and 0.074 nm for the Sm^{3+} and Zn^{2+}, respectively [16].

It is interesting to note that the formation of secondary phase Sm_2O_3 caused reduction in intensity of peaks, as observed in the crystal planes (100), (020) and (011). The same happened in Rani et work. al. in his research depositing doped ZnO films with Nd^{3+} was performed by synthesis by spray pyrolysis, XRD patterns showed that when a new peak by doping 5 mol% of Nd^{3+} was the formation of oxide neodymium, and the intensities of the diffraction peaks (200) and (110) the doped ZnO film decreases significantly compared

to pure ZnO sample [17]. The reduction in intensity occurred along with increasing the mean peak height width. This fact is associated with a reduction in crystallite size [18]. For more information on crystallite size, the Scherrer's equation was used, as shown in equation 2 [19]. Where β is the full width at half maximum of the main peak in XRD pattern. The estimated values for crystallite size are shown in table 1.

$$D = \frac{K\gamma}{\beta cos\theta} \quad (2)$$

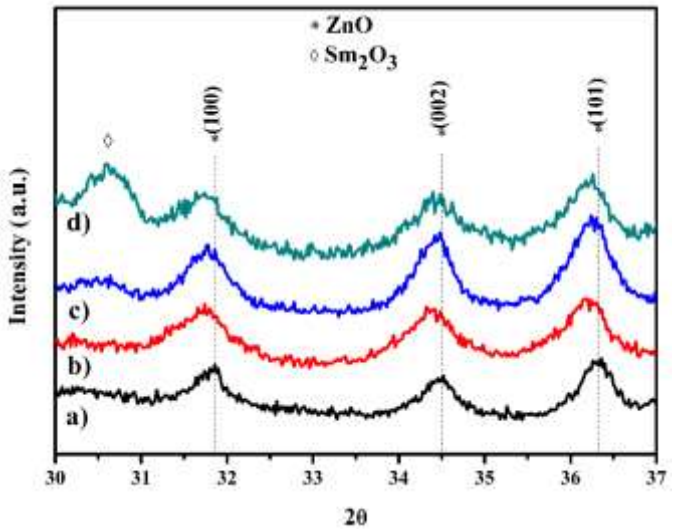

Figure 1: XRD patterns of ZnO:xSm thin film X-ray obtained by spin coating: (a) x = 0, (b) x = 1, (c) x = 2 and (d) x = 4 %mol.

Table 1: Crystalyte size and thickness of the ZnO:xSm (x = 0, 1, 2 and 4 %mol) thin films.

ZnO:xSm thin films	Crystallite size (nm)	Thickness thin films (nm)
x = 0%	13.5	367.7
x = 1%	12.8	354.5
x = 2%	11.8	360.7
x = 4%	9.5	361.3

Fig. 2 shows the micrographs obtained by AFM. It is possible to observe the formation of grains grown and homogeneously distributed on the surface of the thin films, where this growth is associated to the time and temperature used in calcination [20]. The increase of the samarium concentration promotes the growth of the particles on the surface of the films. Fig. 3 shows the histograms referring to the average diameters of the ZnO particles on the surface of the films, where the mean particle size of ZnO follows the order: ZnO:1%Sm < ZnO < ZnO:2%Sm < ZnO:4%Sm. The addition of samarium at concentrations above 1% provides a greater number of defects, which imply the local energetic increase that acts as a driving force for growth with the calcination temperature [21].

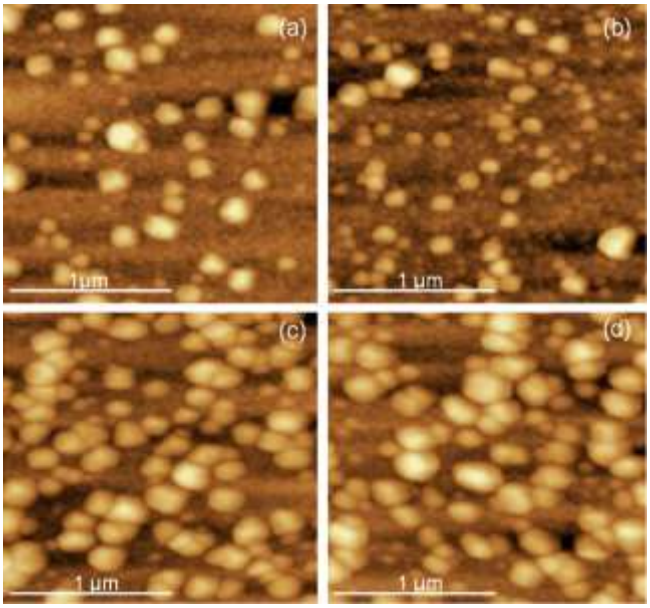

Figure 2: AFM images of ZnO:xSm thin films obtained by spin coating method: (a) x = 0, (b) x = 1, (c) x = 2 and (d) x = 4 %mol.

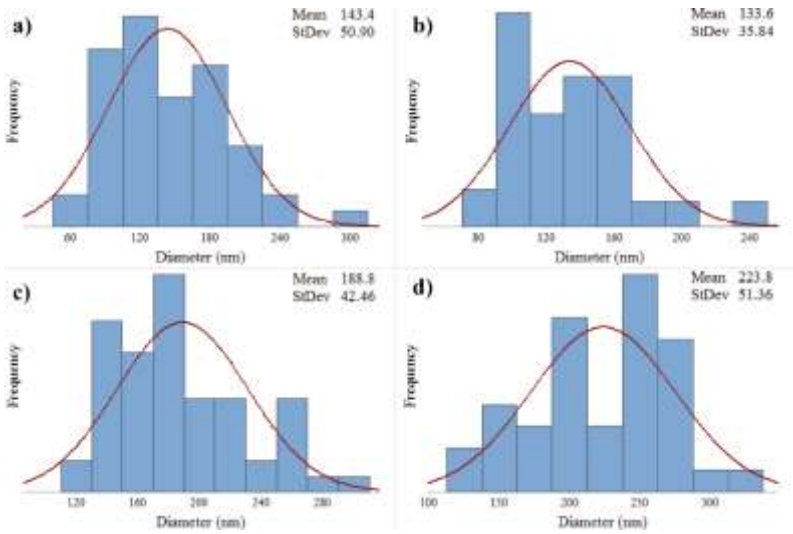

Figure 3: Histogram of the average particle diameters on the surface of the thin films.

The surface and cross aspects of the films were examined by FE-SEM. Fig. 4a presents the surface image of the thin film of pure ZnO, where the presence of small pores on its surface is noticed and that the grains present hexagonal aspect. The appearance of hexagonal grains on the surface of ZnO thin films is reported in other works [22]. According Nayeri *et al*. [23], the grain growth on the surface occurs due to the high energy applied to the system, where the larger grains grow through the coalescence of smaller grains. The measured thicknesses of the thin films ZnO:xSm (with x = 0, 1, 2 and 4 %mol) are shown in table 1. Fig. 4b shows the cross section of the ZnO:4%Sm, indicating that the thin film obtained by spin coating and calcined at 700°C is uniform and dense. As can be seen in table 1, the films have thicknesses in the range of 354.5 to 367.7 nm.

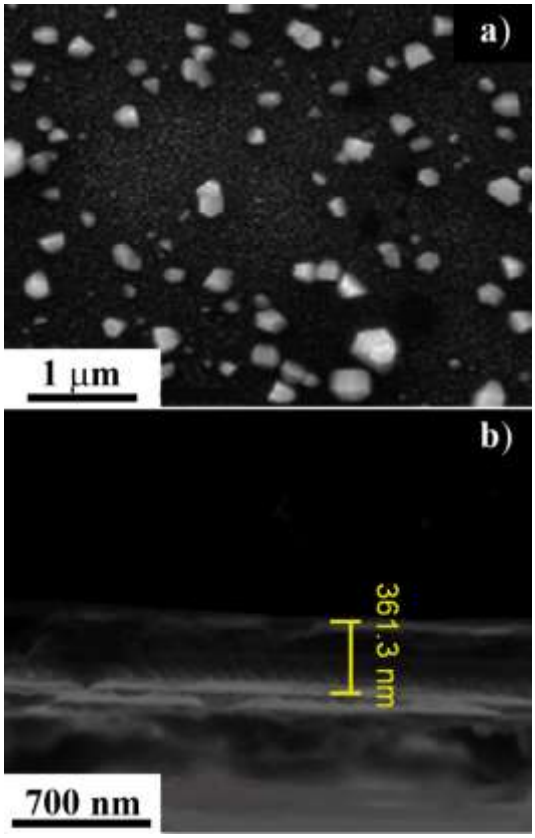

Figure 4: FE-SEM micrograph of (a) surface and (b) cross section of ZnO:4%Sm thin film.

The optical gap was obtained by extrapolating the linear region of the curve according to the Wood and Tauc method [24]. The main changes in the value of the energy of the optical band gap (E_{gap}) can be correlated with the reduction or creation of structural defects or states located within the prohibited area, which may decrease or increase the intermediate energy levels. The band gap energy values Egap were calculated and shown in Fig. 5. The calculated band gap energy of ZnO films varies from 3.57 eV to 3.60 eV, indicating that with increasing concentration of the dopant, there was a slight increase in the energy band of these films. Chen *et al*. [25] reported that the band gap effects are directly related to the film thickness and the crystallite size of the material. As shown, the increase in Sm concentration reduces the crystallite size and the thickness of the thin films, increase their gap energy. The reductions in crystallite size and film thickness with the incorporation of rare earth ions, followed by the small increase in gap energy is widely discussed in the literature [26, 27].

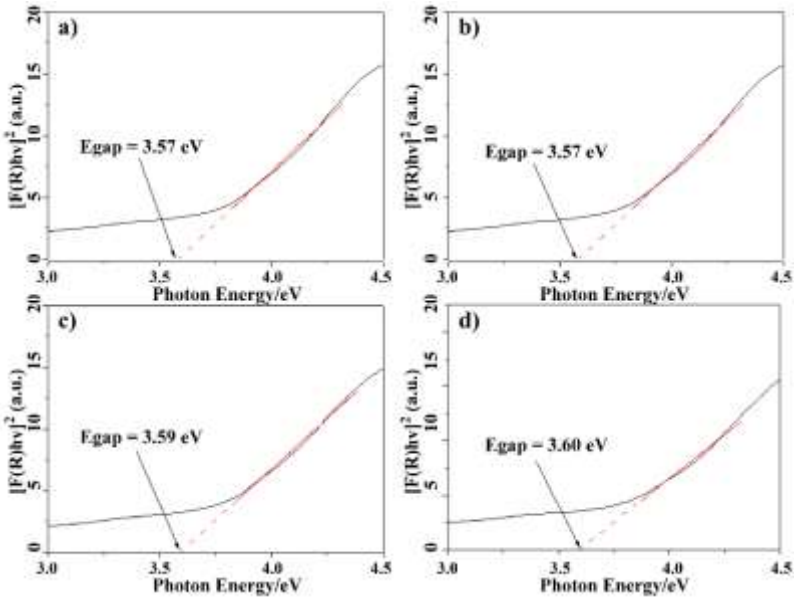

Figure 5: UV-vis spectra of ZnO:xSm films (a) x = 0, (b) x = 1, (c) x = 2 and (d) x = 4 %mol.

Generally, in the optical absorption, the electrons near the edge of the valence band become excited to the bottom of the conduction band due to gap energy [28]. During this transition process, if these electrons encounter disorder, it causes density of their states ρ(hν), where hν is the photon energy, tailing into the energy gap. This tail of ρ(hν) extending into the energy band gap is termed as Urbach tail [29]. We used a linear curve fitting to obtain the Urbach tail, which is defined as the width of the localized states available in the optical band gap that affects the optical band gap structure and optical transitions. The Urbach tail is determined by the following equation 3 [29]:

$$\alpha = \alpha_0 exp \frac{E}{E_U} \qquad [3]$$

Where: α is optical absorption, E is the photon energy, (α_o) is constant and E_U is the Urbach energy, which refers to the width of the exponential absorption edge [29]. The value of E_U was calculated from the slope, and the obtained values are given in Table 2, which indicates that no major changes occurred, as well as band gap values.

Table 2: Urbach energy for ZnO:xSm (x = 0, 1, 2 and 4 %mol) thin films.

ZnO:xSm thin films	Urbach energy (eV)
x = 0%	0.416
x = 1%	0.443
x = 2%	0.436
x = 4%	0.410

ZnO is a class of semiconductor enriched with lattice defects, such as zinc vacancy (V_{Zn}), zinc interstitial (Zn_i), oxygen vacancy (V_O), and oxygen interstitial (O_i). Similarly, the dopants can introduce defects to the ZnO [30]. The cationic substitution of Zn^{2+} by Sm^{3+} can cause many structural, morphological, optical and photocatalytic changes, such as the lattice parameter, gap, grain size, active defect sites and visible light absorption. It is known that the catalytic activity of ZnO nanoparticles doped with lanthanide ions is greater than that of pure ZnO [31]. The doping process with lanthanide ions effectively suppress electron-hole recombination and produce excess free radicals necessary for degradation [6]. These radicals are strong oxidizing agents to degrade refractory organic compounds such as organic dyes and convert them into harmless materials such as H_2O and CO_2 [32]. The catalytic activities of Sm doped ZnO were evaluated by the degradation of aqueous methylene blue. Methylene blue dye is widely used in the textile industry [4].

Fig. 6 shows photocatalytic activity of ZnO:xSm^{3+} (x = 0, 1, 2 and 4 %mol). The photolysis curves were plotted without the presence of catalyst. The degradation efficiency of pure and Sm doped ZnO films for an irradiation time of 420 min was measured to be ZnO = 89.3%, ZnO:1%Sm^{3+} = 90.4%, ZnO:2%Sm^{3+} = 88.1% and ZnO:4%Sm^{3+} = 68.2% while photolysis reduced only 3.1%. The increase in photocatalytic activity for the ZnO:1%Sm^{3+} sample is associated with the introduction of intermediate levels in the ZnO conduction band [33]. The reduction of photocatalytic activity for doping above 1% Sm^{3+} may be associated with reduction of anionic vacancy and excess cationic vacancy generated by the substitution of Zn^{2+} by Sm^{3+}. In addition, Sm_2O_3 phase formation reduces the photocatalytic activity of ZnO. The photocatalytic activity may also be associated with the concentration and size of the ZnO particles on the films surface. As observed through the AFM images, the ZnO:1%Sm^{3+} sample has the smallest mean particle size, consistent with the photocatalytic results. The TOC tests indicated that ZnO, ZnO:1%Sm^{3+}, ZnO:2%Sm^{3+}, ZnO:4%Sm^{3+} samples and the photolysis reduced the amount of organic carbon by 80.1, 84.7, 78.3 and 1.4%.

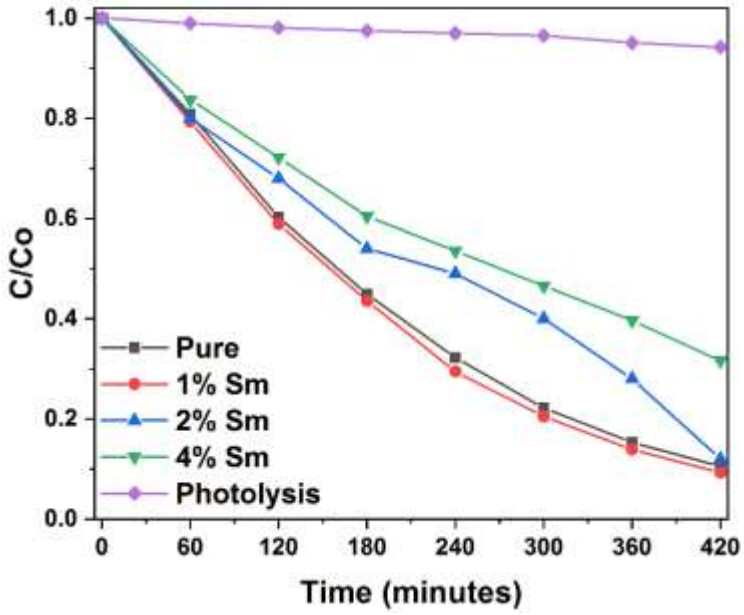

Figure 6: Photocatalytic degradation of the ZnO:xSm (x = 0, 1, 2 and 4 %mol) thin films.

Recycles and maintaining high photocatalytic activity are critical issues for long-term use in practical applications of the catalyst. Therefore, two criteria are required to be considered: (i) the stability of the catalyst to maintain its high activity over time [28] and (ii) the ease with which the catalyst could be recycled from solution [34]. Fig. 7 shows the reuse curves for pure and Sm doped ZnO films. According to Fig. 7, the photocatalytic activity of ZnO reduces its efficiency with the course of the reuse. Efficiency reduces from 89.3 to 77% at the end of the third cycle. Yassitepe *et al.* [1] reported that the photocatalytic activity of ZnO film gradually decreased, but if the photocatalyst are stored in the dark overnight, the photocatalyst activity can be recovered. Doping with Sm gives a lower efficiency reduction with the course of the reuse. The film with 1% Sm reduces from 90.4 to 83.4% and the film with 2% Sm reduces from 88.1 to 84.4%. Thus, the sample with 2% Sm presents the best photocatalytic activity after the third cycle of use, indicating that the incorporation of Sm increases the stability of the catalyst. As shown in Fig. 2, the increase in Sm concentration generates larger grains on the surface of the films. Larger grains have lower surface energy, interacting less with the dye molecules, maintaining the photocatalytic activity after more cycles [35]. The use of films instead of particles facilitates their reuse, avoiding the need for complex treatments for the non-release of particulates as residue. In addition, nanoparticles are difficult to separate, making the process impracticable on larger scales.

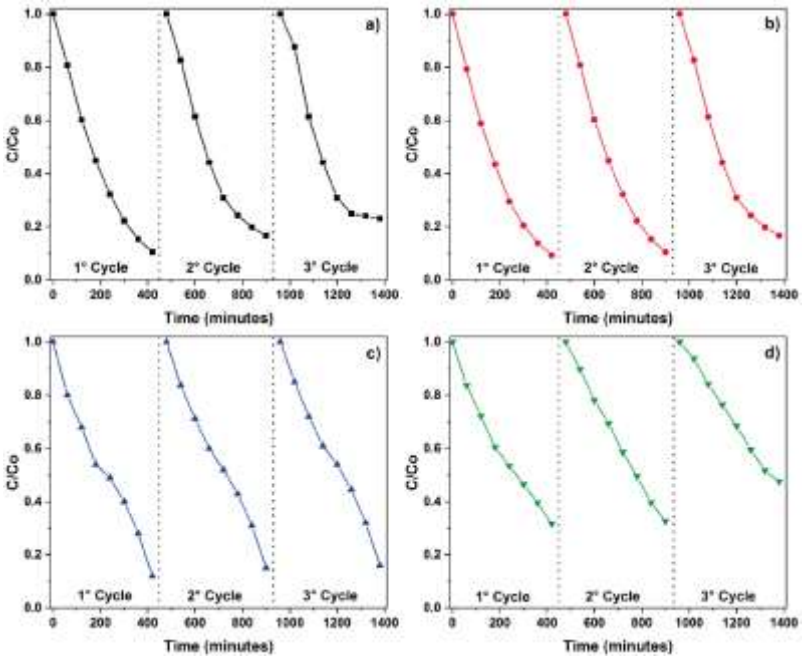

Figure 7: Cycling degradation curve for ZnO:xSm thin films obtained by spin coating method: (a) x = 0, (b) x =

1, (c) x = 2 and (d) x = 4 %mol.

4.CONCLUSIONS

ZnO:xSm3+ (x = 0, 1, 2 and 4 %mol) thin films were successfully obtained by the Complex Polymerization Method (CPM) and spin coating. XRD analysis is showed that the thin film samples have wurtzite structure, presenting the formation of secondary phase only for ZnO:4%Sm sample. FE-SEM illustrate that the thin films of ZnO produced by CPM method have a homogeneous and dense characteristic. The incorporation of Sm3+ into the ZnO lattice provides the reduction of the crystallite size and thickness of the thin films, in addition to generating a slight increase in gap energy. The sample with 1% Sm shows a smaller particle size on the surface of the film, thus having the best photocatalytic activity. Larger particles on the surface of thin films make them more stable, where the sample with 2% Sm presented better reuse property. The appearance of the Sm2O3 phase reduced the activity of the thin film obtained with 4% Sm.

5.ACKNOWLEDGMENTS

The authors thank the financial support of the Brazilian research financing institutions: CAPES/PROCAD 2013/2998/2014 and CNPq No 307546/2014-4.

6.BIBLIOGRAPHY

[1] YASSITEPE, E., YATMAZ, H.C., ÖZTÜRK, C.K. *et al.*, "Photocatalytic efficiency of ZnO plates in degradation of azo dye solutions", *Journal of Photochemistry and Photobiology A: Chemistry*, v. 198, pp. 1-6, 2008.

[2] WANOTAYAN,T., PANPRANOT,J., QIN, J., *et al.*, "Microstructures and photocatalytic properties of ZnO films fabricated by Zn electrodeposition and heat treatment", *Materials Science in Semiconductor Processing*, v. 74, pp. 232-237, 2018.

[3] SÁNCHEZ, C., DORIA, J., PAUCAR, C., *et al.*, "Nanocystalline ZnO films prepared via polymeric precursor method (Pechini)", In: *Physica B: Condensed Matter*, v. 405, pp. 3679-3684, 2010.

[4] HE, G., CAI, J.H., NI, G., "ZnO thin films prepared by a modified water-based Pechini method", *Materials Chemistry and Physics*, v. 110, pp. 110-114, 2008.

[5] POONGODI, G., KUMAR, R.M., JAYAVEL, R., "Structural, optical and visible light photocatalytic properties of nanocrystalline Nd doped ZnO thin films prepared by spin coating method", *Ceramics International*, v. 41, pp. 4169-4175, 2015.

[6] LI, D., XIONG, K., YANG, Z., *et al.*, "Process intensification of heterogeneous photocatalysis with static mixer: Enhanced mass transfer of reactive species", *Catalysis Today*, v. 175, pp. 322-327, 2011.

[7] JAIN, N., BHARGAVA, A., PANWAR, J., "Enhanced photocatalytic degradation of methylene blue using biologically synthesized "protein-capped" ZnO nanoparticles", *Chem. Eng. J.*, v. 243, pp. 549-555, 2014.

[8] KARUNAKARAN, C., RAJESWARI, V., GOMATHISANKAR, P., "Antibacterial and photocatalytic activities of sonochemically prepared ZnO and Ag–ZnO", *Journal of Alloys and Compounds*, v. 508, pp. 587-591, 2010.

[9] FAZIO, E., PATANÈ, S., SCIBILIA, S., e*t al.*, "Structural and optical properties of pulsed laser deposited ZnO thin films", *Current Applied Physics*, v. 13, pp. 710-716, 2013.

[10] PRZEZDZIECKA, E., STACHOWICZ, M., LISOWSKI, W., *et al.*, "The chemical states of As 3d in highly doped ZnO grown by Molecular Beam Epitaxy and annealed in different atmospheres", *Thin Solid Films*, v. 605, pp. 283-288, 2016.

[11] MAEJIMA, K., KOIDA, T., SAI, H., *et al.*, "Influences of deposition temperature on characteristics of B-doped ZnO films deposited by metal–organic chemical vapor deposition", *Thin Solid Films*, v. 559, pp. 83-87, 2014.

[12] BU, I.Y., "Enhanced photocatalytic activity of sol–gel derived ZnO via the co-doping process", *Superlattices and Microstructures*, v. 86, pp. 36-42, 2015.

[13] TARWAL, N.L., PATIL, P.S., "Enhanced photoelectrochemical performance of Ag–ZnO thin films synthesized by spray pyrolysis technique", *Electrochimica Acta*, v. 56, pp. 6510-6516, 2015.

[14] CAI, J.H., NI, G., HE, G., *et al.*, "Red luminescence in ZnO films prepared by a glycol-based Pechini method", *Physics Letters A*, v. 372, pp. 4104-4108, 2008.

[15] MIAO, J., JIA, Z., LU, H.-B., *et al.*, "Heterogeneous photocatalytic degradation of mordant black 11 with ZnO nanoparticles under UV–Vis light", In: *Journal of the Taiwan Institute of Chemical Engineers*, v. 45, pp. 1636-1641, 2014.

[16] PIAO, J., TSENG, L.-T., YI, J., "Ferromagnetism in Sm doped ZnO nanorods by a hydrothermal method", *Chemical Physics Letters*, v. 649, pp. 19-22, 2016.

[17] DEEPA RANI, T., TAMILARASAN, K., ELANGOVAN, E., *et al.*, "Structural and optical studies on Nd doped ZnO thin films", *Superlattices and Microstructures*, v. 77, pp. 325-332, 2015.

[18] ANDRADE NETO, N.F., OLIVEIRA, Y.G., PASKOCIMAS, C.A., *et al.*, "Increase of antimicrobial and photocatalytic properties of silver-doped PbS obtained by sonochemical method", *Journal of Materials Science: Materials in Electronics*, v. 28, pp. 19052–19062, 2018.

[19] ALSEBAIE, D.M., SHIRBEENY, W., ALSHAHRIE, A., *et al.*, "Ellipsometric study of optical properties of Sm-doped ZnO thin films Co-deposited by RF-Magnetron sputtering", In: *Optik - International Journal for Light and Electron Optics*, v. 148, pp. 172-180, 2017.

[20] KAJIKAWA, Y., "Texture development of non-epitaxial polycrystalline ZnO films", In: *Journal of Crystal Growth*, v. 289, pp. 387-394, 2006.

[21]] KELLY, M.N., RHEINHEIMER, W., HOFFMANN, M.J., *et al.*, "Anti-thermal grain growth in SrTiO3: Coupled reduction of the grain boundary energy and grain growth rate constant", In: *Acta Materialia*, v. 149, pp. 11-18, 2018.

[22] HE, H.Y., FEI, J., LU, J., "Sm-doping effect on optical and electrical properties of ZnO films", In: *Journal of Nanostructure in Chemistry*, v. 5, pp. 169-175, 2015.

[23] DEHGHAN NAYERI, F., KOLAHDOUZ, M., ASL-SOLEIMANI, E., *et al.*, "Low temperature carving of ZnO nanorods into nanotubes for dye-sensitized solar cell application", In: *Journal of Alloys and Compounds*, v. 633, pp. 359-365, 2015.

[24] WOOD, D.L., TAUC, J., "Weak Absorption Tails in Amorphous Semiconductors", In: *Physical Review B*, v. 5, pp. 3144-3151, 1972

[25] CHEN, W.-F., CHEN, H., KOSHY, P., *et al.*, "Effect of doping on the properties and photocatalytic performance of titania thin films on glass substrates: Single-ion doping with Cobalt or Molybdenum", In: *Materials Chemistry and Physics*, v. 205, pp. 334-346, 2018.

[26] GIL-ROSTRA, J., YUBERO, F., FERRER, F.J., *et al.*, "Combined reactive magnetron sputtering and plasma decomposition of non-volatile precursors to grow luminescent thin films", In: *Surface and Coatings Technology*, v. 222, pp. 144-150, 2013.

[27] GIL-ROSTRA, J., FERRER, F.J., MARTÍN, I.R., *et al.*, "Cathode and ion-luminescence of Eu:ZnO thin films prepared by reactive magnetron sputtering and plasma decomposition of non-volatile precursors", In: *Journal of Luminescence*, v. 178, pp. 139-146, 2016.

[28] BOUBAKER, K., "A physical explanation to the controversial Urbach tailing universality", In: *The European Physical Journal Plus*, v. 126, pp. 10, 2011.

[29] URBACH, F., "The Long-Wavelength Edge of Photographic Sensitivity and of the Electronic Absorption of Solids", In: *Physical Review*, v. 92, pp. 1324-1324, 1953.

[30] WANG, Y., PIAO, J., LU, Y., *et al.*, "Intrinsic ferromagnetism in Sm doped ZnO", In: *Materials Research Bulletin*, v. 83, pp. 408-413, 2016.

[31] ZSILÁK, Z., SZABÓ-BÁRDOS, E., FÓNAGY, O., *et al.*, "Degradation of benzenesulfonate by heterogeneous photocatalysis combined with ozonation", In: *Catalysis Today*, v. 230, pp. 55-60, 2014.

[32] PANDIYARAJAN, T., MANGALARAJA, R.V., KARTHIKEYAN, B., *et al.*, "UV-A light-induced photodegradation of Acid Blue 113 in the presence of Sm-doped ZnO nanostructures", In: *Applied Physics A*, v. 119, pp. 487-495, 2015.

[33] LU, Y., LIN, Y., XIE, T., *et al.*, "Enhancement of visible-light-driven photoresponse of Mn/ZnO system: photogenerated charge transfer properties and photocatalytic activity", In: *Nanoscale*, v. 4, pp. 6393-6400, 2012.

[34] SIN, J.-C., LAM, S.-M., LEE, K.-T., *et al.*, "Preparation and photocatalytic properties of visible light-driven samarium-doped ZnO nanorods", In: *Ceramics International*, v. 39, pp. 5833-5843, 2013.

[35] UZDIN, V.M., POTKINA, M.N., LOBANOV, I.S., *et al.*, "Energy surface and lifetime of magnetic

skyrmions", In: *Journal of Magnetism and Magnetic Materials*, v. 459, pp. 236-240, 2018.

ORCID

Nivaldo Freire de Andrade Neto https://orcid.org/0000-0003-1421-2904
Raquel Guilherme de Carvalho https://orcid.org/0000-0003-1620-5636
Laurênia Martins Pereira Garcia https://orcid.org/0000-0003-0194-0427
Rubens Maribondo Nascimento https://orcid.org/0000-0001-9094-0044
Carlos Alberto Paskocimas https://orcid.org/0000-0002-1915-4291
Elson Longo https://orcid.org/0000-0001-8062-7791
Maurício Roberto Bomio Delmonte https://orcid.org/0000-0001-9016-4217
Fabiana Villela da Motta https://orcid.org/0000-0002-3523-737X